PILOT-IN-THE-LOOP INFLUENCE ON CONTROLLED TILTROTOR STABILITY AND GUST RESPONSE

J. Serafini, D. Muro, M. Gennaretti
***University Roma Tre,**
Via della Vasca Navale 79, 00146, Roma, Italy

Keywords: *tiltrotor, rotocraft-pilot coupling, gust alleviation, stability*

Abstract

This work is aimed at the study of influence of the tiltrotor-pilot coupling on both aeroelastic stability and gust response, when the rotorcraft is subject to the action of a control system devoted to alleviate gust effects. To this purpose, first the wing-proprotor aeroelastic model has been coupled with the rigid-body dynamics equations for the identification of the control law, and then the validation analysis has been accomplished by introducing in the loop a model of the pilot behaviour. Helicopter and airplane mode configurations have been examined showing that rotorcraft-pilot coupling effects are not critical in terms of gust response (controlled or uncontrolled), while their interaction with AFCS may cause the insurgency of instabilities in airplane-mode flight.

1 Introduction

The study of the effects of pilot presence in aircraft dynamics is a field of research of growing interest during the last two decades. However, it is still relatively unexplored, despite the fact that adverse interactions are documented since early years of flight history. In the past, these interactions were usually classified as pilot errors or inability to operate under particular flight conditions, as it is proven by the results of the investigations about numerous flight accidents (see, for instance, Ref. [3]). This lack of knowledge was expecially true for rotorcraft, which have been studied from this point of view since 80's. In these years several reports of rotorcraft accident ascribed to anomalous interaction between pilot and helicopters have been released, like that of a Swiss AB204B helicopter that hit hardly the ground after a sequence of vertical oscillations arisen after the drop of the load [3]; however, other cases (with smaller consequences) have been reported, thus pointing out that there is a risk of potential instabilities for safe-supposed helicopters. The first answers to this problem proposed by manufacturers have been given in terms of piloting warning and prescritions often consisting of stop grasping controls. However it appears evident that developing tools for safe helicopter design is a major interest in the future.

The authors focused part of their research activity on Rotorcraft-Pilot Coupling (RPC) since 2005, and developed several models to predict their insurgency (see, for instance, Refs [12, 1, 16, 17, 11]). In particular they studied the so called PAOs (Pilot Assisted Oscillations) and the corresponding aeroelastic modelling requirements. The PAOs are classified as unintentional interactions between pilot and aircraft, with a distinctive frequency above 2Hz; under this value it is usual to refer to RPC as PIOs (Pilot Induced Oscilations), with the different naming remarking the role of pilot in the phenomena. Indeed, the consciousness of the action of a human being on controls is predominant up to about $1-2$Hz, while above this value the main effect of the presence of the pilot is a transfer of vibrations from the seat to sticks and pedals, like the one produced by a system of masses and impedences, resulting essentially non behavioral.

From the aircraft modelling point of view, an analogous classification can be formulated: up to 1Hz the most influencing dynamics are those related to flight mechanics and related phenomena are referred to as rigid-body RPC; for higher values of frequency elasticity and servoelasticity play a dominant role, and related phenomena are referred to as aeroelastic RPC. However, due to periodicity and nonlinearity of rotorcraft dynamics, it is impossible to completely separate the two ranges of frequency.

While first recognized RPCs were exclusively related to aeroelastic dynamics and biodynamics with the possible influence of servoleasticity, since Automatic Flight Control Systems became more and more prominent in modern aircraft, new threat of adverse RPC arises both in rigid-body and aeroelastic range of frequency. Indeed, controllers are usually designed without inclusion of pilot models, leaving to flight tests the discovery of possible inefficiency and criticity. In this paper, starting from a tiltrotor AFCS recently developed for gust response alleviation [14] the controller efficiency and robustness is examined in the presence of a passive pilot in the loop, both for deterministic and stochastic gust inputs, in order to have a view of the RPC phenomena resulting from interaction with AFCS. In the following, first the mathematical models applied to simulate tiltorotor aeroelasticity and pilot behavior are shortly presented, and then the results of the numerical investigations concerning a tiltrotor in helicopter and airplane mode flight are discussed.

2 Tiltrotor Model for Gust Response

The mathematical model for the simulation of tiltrotor aeroelasticity under vertical gust action is obtained by coupling longitudinal rigid-body motion equations with wing-proprotor aeroelastic equations. Wing and proprotor blades are described as bending-torsion beam-like structures that are coupled with gimbal dynamics, longitudinal rigid-body motion, and the variables involved in the control action.

2.1 Proprotor Model

The introduction of proprotor blades aeroelastic model is necessary because these are slender structures that undergo not negligible deformations that, in turn, affect the dynamic behavior of the complete rotorcraft. The proprotor blades aeroelastic model applied in this work is based on the nonlinear bending-torsion structural formulation presented in Ref. [8], that is valid for straight, slender, homogeneous, isotropic, nonuniform, twisted blades, undergoing moderate displacements. Blade dynamics equations are forced by inertial loads due to gimbal, wing and rigid-body dynamics and by the aerodynamic loads.

The aerodynamic loads are evaluated through two-dimensional, quasi-steady models with wake-inflow corrections (mainly, to take into account trailing vortices effect). These are based on low-frequency approximation of Theodorsen and Greenberg theories [18, 7], with the lift deficiency function assumed to be constant and equal to one (see, for instance, Ref. [5]). This limitation implies that the effects of unsteady shed vortices on the theoretical solutions are neglected, thus simplifying the identification of the linearized perturbation system, in that avoiding the introduction of finite-state modelling of aerodynamic loads.

2.2 Wing Model

Akin to proprotor blades, wing structure is described as a bending-torsion beam-like model derived from Ref. [8]. It is composed of a set of three partial differential equations forced by section aerodynamic loads described by the low-frequency approximation of Theodorsen theory [18], as well as the forces and moments transmitted by the pylon/gimbal/proprotor system at the wing section where the pylon is attached to (see, for instance, Ref. [6]).

2.3 Rigid-Body Motion Equations

Under the assumption of atmospheric disturbances acting in the plane of symmetry, the rigid-body motion of the rotorcraft is described in terms of the velocity perturbations along longitudinal axis, u, yawing axis, w, and perturbation of pitch angular velocity, q. Then, the longitudinal-motion ordinary differential equations written in stability axes read (see, for instance, Ref. [2])

$$\begin{aligned}\bar{m}\,\dot{u} &= -\bar{m}\,g\,\theta + \Delta X\\ \bar{m}\,\dot{w} &= \bar{m}\,U\,q - \bar{m}\,g\,\theta + \Delta Z\\ J\,\dot{q} &= \Delta M\end{aligned}$$

with θ denoting pitch angle perturbation, and $\dot{\theta} = q$. In the equations above, $\bar{m}$ is the mass of the aircraft, J is the aircraft moment of inertia around the stability lateral y-axis, U is the tiltrotor velocity in trimmed unperturbed conditions, while $\Delta X, \Delta Z$ and ΔM are the aerodynamic force and moment perturbations in disturbed flight, with the additional contribution from wing-proprotor inertial loads due to elastic deformations.

2.4 Linearized Aeroelastic System

For the sake of synthesis of control laws aimed at alleviation of responses to atmospheric perturbations, it is convenient to identify the first-order, linearized, ordinary differential equation model of the gust response problem (plant model). In order to obtain it, first the partial differential equations (namely, those describing blade and wing dynamics) are integrated spatially through the Galerkin method, by expressing the dofs as linear combinations of Lagrangean coordinates with appropriate shape functions [5]. Then the contributions to the aeroelastic matrices of the linearized small perturbation model, if not explicitly appearing in blade and wing equations as linear terms, are determined by numerical differentiation about the trimmed equilibrium flight condition. For instance, for q_j^b denoting the j-th blade Lagrangean coordinate, mass, damping and stiffness matrices of the blade perturbation equations are obtained by

$$M_{ij}^b = -\left.\frac{\partial f_i^b}{\partial \ddot{q}_j^b}\right|_{eq}, \quad C_{ij}^b = -\left.\frac{\partial f_i^b}{\partial \dot{q}_j^b}\right|_{eq}, \quad K_{ij}^b = K_{ij}^{b,lin} - \left.\frac{\partial f_i^b}{\partial q_j^b}\right|_{eq}$$

with $K_{ij}^{b,lin}$ denoting the contribution from linear explicit terms, while f_i^b is the i-th generalized force resulting from the combination of aerodynamic loads, inertial loads and nonlinear structural terms. The same technique is applied also to determine matrices of the perturbation contributions from wing, gimbal (if present) and rigid-body motion coupling terms, as well as the terms in the control matrix, $\hat{\mathbf{B}}^b$, and the input matrix, $\hat{\mathbf{F}}^b$.

The application of this procedure also to wing, gimbal (if present), and rigid-body motion equations, and then re-arranging the resulting set of linear equations in state-space form yields

$$\dot{\mathbf{x}} = \mathbf{A}\,\mathbf{x} + \mathbf{B}\,\mathbf{u}_c + \mathbf{F}\,\mathbf{v}_a \tag{1}$$

where $\mathbf{x}$ is the vector of the system state variables, $\mathbf{u}_c$ is the vector of the control variables, $\mathbf{v}_a$ is the vector of the gust velocity components, while $\mathbf{A}$ is obtained as a combination of mass, damping, and stiffness matrices, and $\mathbf{B}$ and $\mathbf{F}$ are derived from $\hat{\mathbf{B}}$'s and $\hat{\mathbf{F}}$'s, respectively. Note that when the configuration examined is such that time-periodic matrices appear, multiblade coordinates are introduced and constant-matrix approximation is applied before deriving the state-space equation form.

3 Gust Alleviation Control System

The closed-loop law that drives the control actuators aimed at gust alleviation is derived from optimal control theory. It yields a feedback controller through minimization of a quadratic performance index, under the constraint to satisfy the linear system dynamics equations. Specifically, for $\mathbf{Q}$ denoting a constant, symmetric, positive semi-definite matrix and $\mathbf{R}$ denoting a constant, symmetric, positive definite matrix, the performance index is defined as

$$J = \frac{1}{2}\int_0^\infty \left(\mathbf{x}^T\,\mathbf{Q}\,\mathbf{x} + \mathbf{u}_c^T\,\mathbf{R}\,\mathbf{u}_c\right)\mathrm{d}t$$

Coupling it with the differential constraint in eq. (1) written for no atmospheric disturbances (they are considered as process noise), calculus of variations yields the following optimal feedback controller

$$\mathbf{u}_c = -\mathbf{R}^{-1}\mathbf{B}^T\mathbf{S}\mathbf{x} \tag{2}$$

where $\mathbf{S}$ is the unique constant, symmetric, positive semi-definite matrix that satisfies the following algebraic Riccati equation

$$\mathbf{A}^T\mathbf{S} + \mathbf{S}\mathbf{A} - \mathbf{S}\mathbf{B}\mathbf{R}^{-1}\mathbf{B}^T\mathbf{S} + \mathbf{Q} = \mathbf{0}$$

The weighting matrices, $\mathbf{Q}$ and $\mathbf{R}$, are defined by the control designer: usually, they are chosen as a trade-off between the effectiveness of control action and control effort required.

As stated in eq. (2), the actuation of the optimal controller requires the knowledge of the entire system state vector, $\mathbf{x}$, but commonly only a subset of state variables (or combinations of them) may be measured. In this case state an estimate from available measurements is needed and an observer has to be introduced.

3.1 Observers for state estimate

Let us assume that the vector of measurements, $\mathbf{y}$, is related to the system state by

$$\mathbf{y} = \mathbf{C}\mathbf{x} + \mathbf{w}$$

where $\mathbf{C}$ is a constant matrix and $\mathbf{w}$ is a white, gaussian, measurement noise. Then, the estimate of the system state, $\mathbf{x}_e$, to be used as input to the control law in eq. (2) may be obtained from the following dynamic observer [4].

$$\dot{\mathbf{x}}_e = \mathbf{A}\mathbf{x}_e + \mathbf{B}\mathbf{u}_c + \mathbf{K}(\mathbf{y} - \mathbf{C}\mathbf{x}_e) \tag{3}$$

For $\mathbf{K} = \mathbf{P}\mathbf{C}^T\mathbf{W}^{-1}$, with $\mathbf{P}$ solution of the following algebraic Riccati equation

$$\mathbf{A}\mathbf{P} + \mathbf{P}\mathbf{A}^T - \mathbf{P}\mathbf{C}^T\mathbf{W}^{-1}\mathbf{C}\mathbf{P} + \mathbf{F}\mathbf{V}\mathbf{F}^T = \mathbf{0}$$

and $\mathbf{W}$ and $\mathbf{V}$ denoting, respectively, spectral density matrices of observation and process noise (the latter also assumed to be white and gaussian), eq. (3) represents the Kalman-Bucy filter that yields the optimal estimation of the state (*i.e.*, the estimate that minimizes the covariance matrix of the error, $\mathbf{x} - \mathbf{x}_e$) (see Ref. [4] for further details). The separation theorem asserts that the compensator obtained as combination of Kalman-Bucy filter with the optimum deterministic control in eq. (2) yields the optimal control law [4]. It is important to remark that $\mathbf{A}$, as usual, is the state matrix of the aircraft without the pilot-in-the-loop. The discrepancy between that and the actual system (with the pilot-in-the-loop) and its effect of control performance and reliability underlie this paper.

4 Biodynamic Pilot Modelling

As stated in Section 1, the pilot actions on controls may be classified in two categories. The first category includes the volutary actions corresponding to commands that are intentionally entered by the pilot to perform some tasks, in response to his perception (which may be correct or not) and his ability (conventionally these actions are considered to be significant up to about 2Hz). Determining a model for this category of actions requires a deep knowledge of behavioural processes, as well as biomechanics, since the limbs have a proper bandwidth.

The second way a pilot may operate on controls are the unintentional actions occurring as mechanical response of his limbs to the excitations coming from the environment (typically, vibrations of seat and cockpit). These phenomena are strictly of biomechanical nature, and are usually modelled by following two different approaches. One consists of a direct simulation of the human body as a set of masses and impedences, while the other takes into account the presence of the pilot through an equivalent transfer function between (typically) seat vibrations and controls, which is identified from experimental data obtained from a shaker or a flight simulator with moving cabin (the main difference between the two methods is that in the simulator, the pilot retains the visual perception of the flight path, which is a significant issue for low frequency response, as we will discuss below). Currently, the approach based on experiments, although speculatively less accurate, is in fact largely employed due to the difficulties in deriving a consistent biomechanic model.

The first work on helicopter-pilot coupling was presented by Mayo [13] in late 80's, while analyses on tiltrotor-pilot coupling started a bit later [15]. Mayo's pilot model is a Single Input Single Output (SISO) model which relates collective pitch control perturbations to seat vibrations and is a well suited tool for pilot-in-the-loop aerolastic analysis. However, it is not only inadequate to simulate the behavioural processes, but also returns a non physical response at low frequencies, in that yields an indefinite growth of collective control in response to zero-frequency input (this behaviour is probably due to the fact that Mayo performed his experiments without pilot visual feedback). While this doesn't represent a problem for stability analysis performed through eigenvalues, it does for a time-marching approach. However, this critical point may be overcome by replacing the two integration poles appearing in the original version of the pilot transfer function suggested by Mayo [13], with two poles at very low frequency 0.1Hz. This yields the following expression for the pilot model

$$\tilde{\alpha}_0 = \frac{G}{r_0}\frac{1}{(s+0.1)^2}\frac{-s(s+8.51)}{s^2+13.7s+452.3}\tilde{a}_s \qquad (4)$$

where a_s represent vertical seat acceleration, α_0 is the collective stick angle and r_0 is the collective lever length. Figure 1 depicts the corresponding magnitude and phase as functions of the frequency, showing that the two poles identified by Mayo [13] are close to 3.5Hz with about 30% damping. Here, the pilot passive (involuntary) action is modelled by the transfer function in eq. (4). Note that in this work a generic tiltrotor has been considered, assuming vertical run for the collective stick (as it is in several cases), but without any specific assumption about cockpit measures and pilot position. Therefore, the value of pilot gain, G, has been arbitrarily chosen for the numerical investigations, in that it was observed by Mayo to be dependent on the pilot arm reference position [13]. In addition, for the sake of

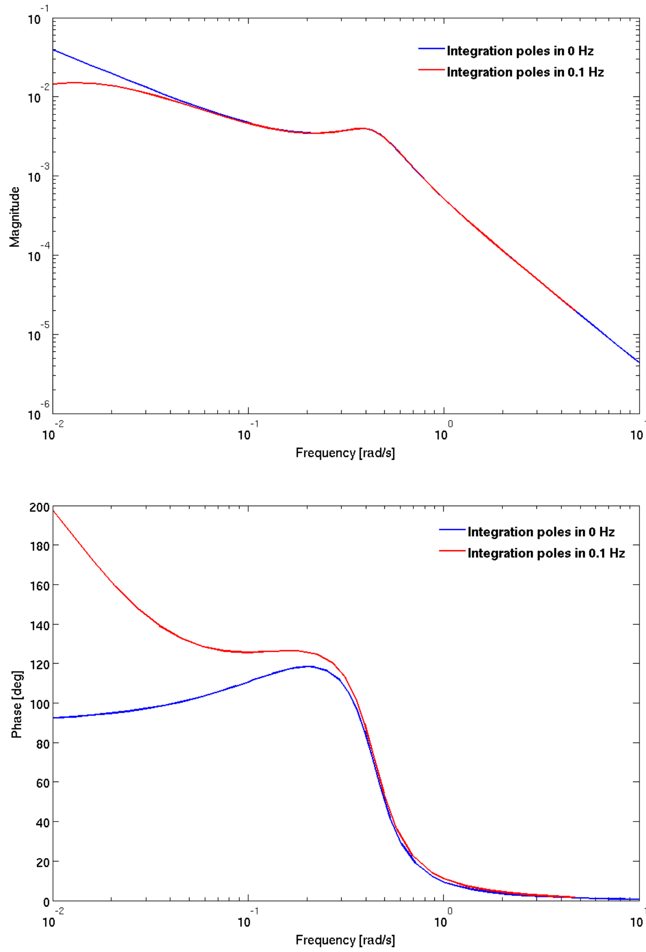

Fig. 1 Pilot transfer function

simplicity rotorcraft-pilot coupling has been limited to arise via collective pitch, although that due to cyclic pitch might also give rise to adverse interaction between pilot and AFCS.

The effects of control chain dynamics on pilot commands have been also included. It is well known that the effect of servoelasticity on aircraft-pilot coupling is a main cause of PIO. This is due to the misleading feedback that the pilot may receive, mainly because of delays and rate limiting [10]. The situation is different in PAOs range, where control dynamics is less influential; however, its introduction leads to a more realistic aeroservoelastic simulation. Here, the collective stick is supposed to control the collective pitch of the rotors with the presence of an impedence (mass-damper) between lever and actuators (a common practice to reduce high frequency inputs). This impedence has been chosen so as to attain a time constant of 0.04s.

The final tiltrotor pilot-in-the-loop aeroelastic system examined in this work may be represented through the block diagram sketched in fig. 2. The input to the system is the gust velocity, along with noise affecting measurements. Two different feedbacks are present: one is from the pilot which acts on collective lever causing a variation of collective pitch; the other is from the estimator-controller block which actuates the control variables.

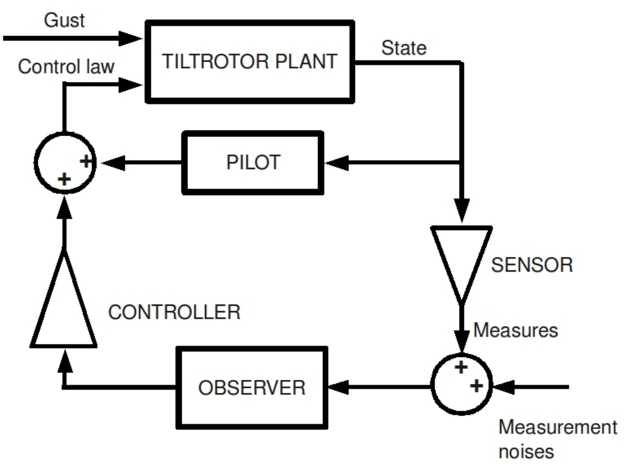

Fig. 2 Block diagram of the aeroelastic loop

5 Numerical results

The numerical investigation concerns the study of the influence of pilot-in-the-loop on tiltrotor stability and gust response, in the presence of a controller devoted to gust effect alleviation. The aircraft examined is a XV15-type tiltrotor. It has two three-bladed, gimballed proprotors with radius $R = 3.82$m, solidity $\sigma = 0.089$, and a rectangular wing with length $L = 5.08$m and aspect ratio equal to 6.6 (see Ref. [9] for further details). Gust encountering in airplane and helicopter mode flights has been analyzed, considering both deterministic and stochastic models for describing the distribution of the atmospheric disturbance. The effects of gust disturbance are examined in terms of vertical load factor at the rotorcraft center of mass. In this analysis the control action is performed by actuation of proprotor collective and longitudinal pitch, wing flaperon and elevator. Note that, in order to simulate the filtering effect of actuators dynamics, a low-pass filter having 100Hz bandwidth has been assumed to be present downstream of the controller.

5.1 Helicopter mode

In the helicopter flight condition examined the proprotor rotational speed is $\Omega = 62.83$rad/s, and the cruise speed is $V_f = 30.84$m/s. First, a pilot gain parametric analysis is performed in order to identify a value which suitable for the following investigation. Considering the uncontrolled tiltrotor load factor response to a vertical step gust, fig. 3 shows the effect of pilot gain, G, ranging from 0 to 1. The presence of the pilot modifies the system eigenvalues, introducing less damped modes that become unstable when $G = 1$. Next results have been obtained using $G = 0.8$, which is a gain value for which the pilot in the loop introduces a slighly damped mode and is reasonable with respect to those identified by Mayo for a helicopter cockpit [13]. As stated in Section 4, the identification of the pilot gain value exactly corresponding to the tiltrotor under examination is well beyond the aims of this

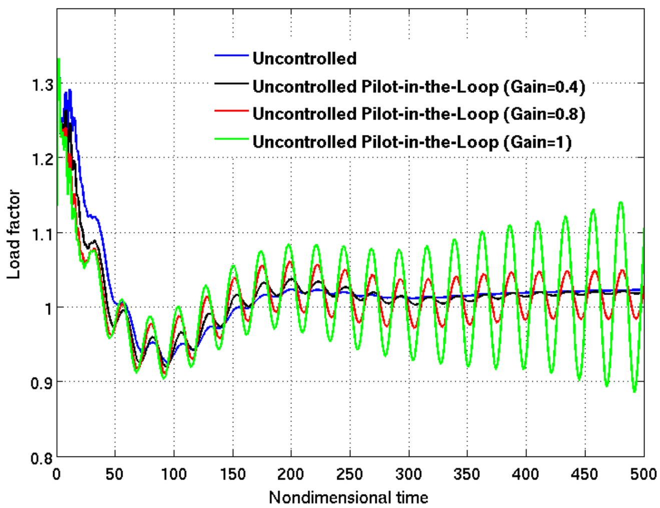

Fig. 3 Effect of pilot gain on response to a step-gust, helicopter mode

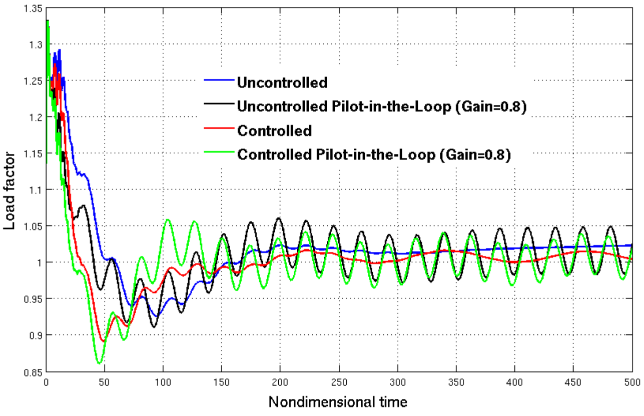

Fig. 4 Controlled step-gust response, helicopter mode

paper; however, the one chosen is representative of the strong coupling typically occurring in rotorcraft configurations. Then, the step-gust re-

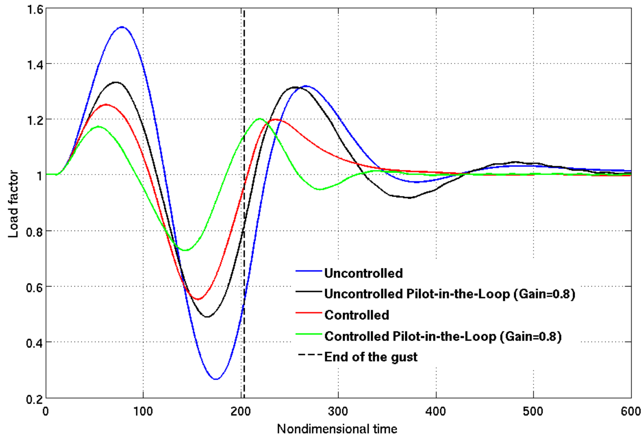

Fig. 5 Load factor due to $1-\cos$ gust, helicopter mode

sponse has been evaluated with and without controller action, with and without pilot in the loop. The results are presented in fig. 4, showing that the presence of the pilot affects uncontrolled and controlled responses in similar ways. Note that in this case the control action is practically uneffective in that it has been designed to be optimal for the $1-\cos$ gust. Next, the controller perfomance has been tested for a vertical $1-\cos$ gust, with length equal to 100m and peak velocity equal to 15.42m/s. The resulting load factors are shown in fig. 5. In this case load factor peaks are significantly reduced by the action of the controller, with the pilot influence tending to be in favour of the attenutation of gust effects (a similar result has been shown in Ref. [17]). Note that the effects of the slightly damped mode introduced by the pilot do not appear in fig. 5, in that hidden by the larger load factor response (however they may be clearly observed as the observation time increases). The actuation effort corresponding

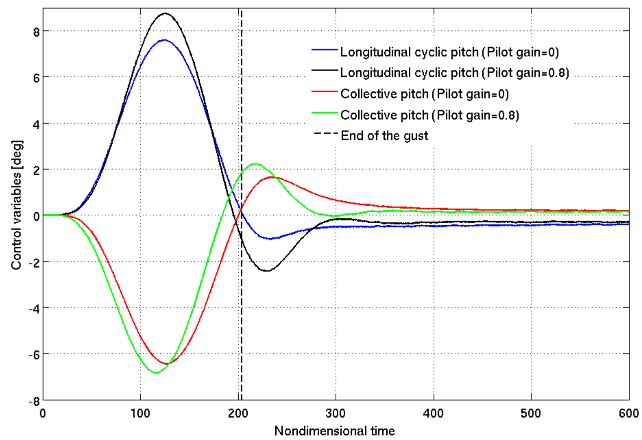

Fig. 6 Rotor controls history

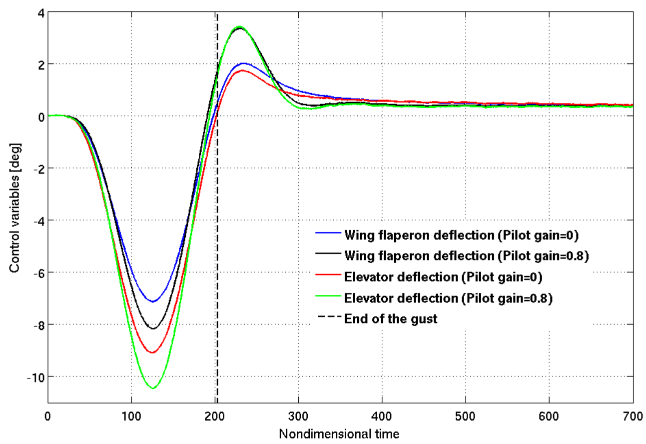

Fig. 7 Flaperon and elevator controls history, helicopter mode

to the controlled response in fig. 5 is illustrated in figs. 6 and 7. These pictures show that, in the case examined, the presence of the pilot induces a small decrease of the rotor control effort, while requiring a bit larger increase of elevator and flaperon contribution. Finally, a stochastic gust encounter has been simulated by the superposition of the $1-\cos$ gust with a white noise, with inclusion of the presence of measurements noise (thus requiring the introduction of the Kalman filter in the control process). As shown in fig. 8, the inclusion of stochastic contributions to the perturbing gust does not affect significantly the responses, although a small loss of controller efficiency is observed. The influence of pilot remains unchanged (see fig. 5 for comparison).

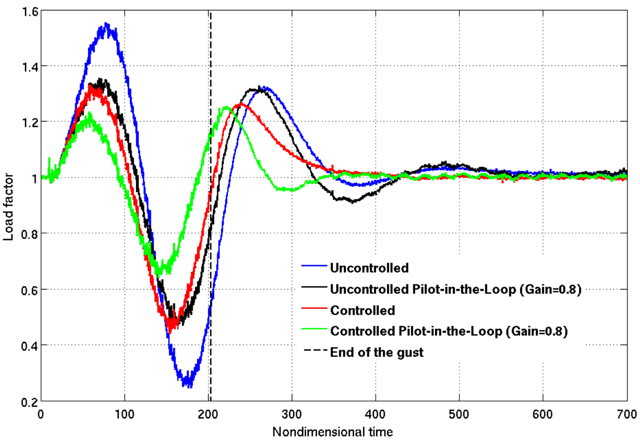

Fig. 8 Load factor due to stochastic gust, helicopter mode

5.2 Airplane mode

The second flight condition examined is an airplane mode, with a cruise velocity of 92.52m/s. With respect to the helicopter-mode flight the main differences are that the gust crossing time is sensibly smaller (thus moving the frequency response toward PAO range), and that a change in collective pitch control results in a longitudinal perturbative force (thus not closing directly the pilot-tiltrotor loop, which is pass through by vertical seat accelerations). Akin to the helicopter-mode case, first a pilot gain sweep has been examined in the presence of a vertical step gust: as shown in fig. 9, also in this configuration the value $G = 0.8$ causes a slightly damped response from the uncontrolled aeroelastic system,

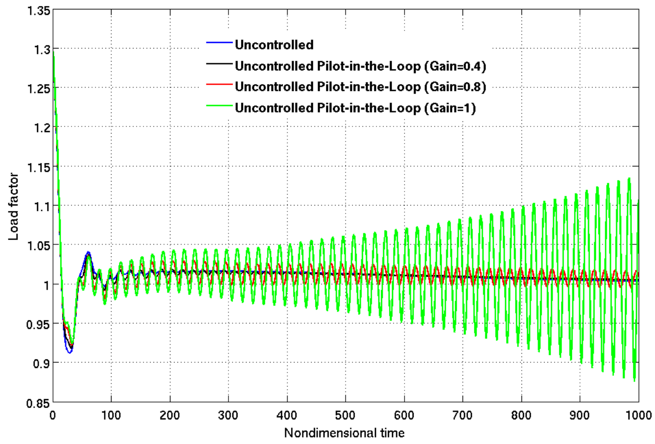

Fig. 9 Effect of pilot gain on response to a step-gust, airplane mode

and hence it has been kept unchanged. Then, the

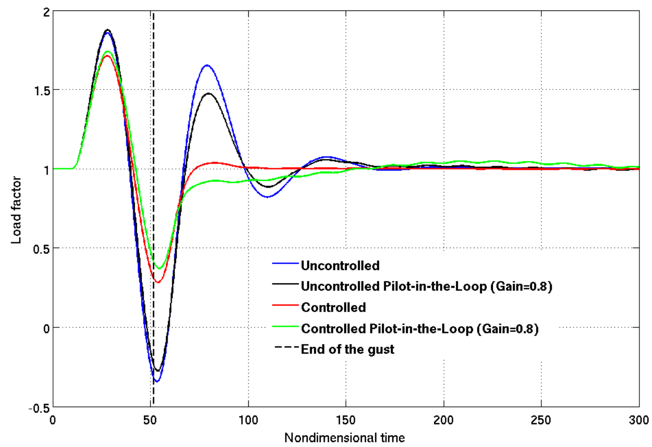

Fig. 10 Load factor due to $1-\cos$ gust, airplane mode

controlled response to the $1-\cos$ vertical gust already considered in helicopter mode is examined. Figure 10 shows that the controller performance is satisfactory and that, as expected, in this case the presence of the pilot in the loop only barely affects the tiltrotor response (both controlled and uncontrolled). As mentioned above, this is due to the fact that perturbation and feedback are“orthogonal” (mainly act on perpedicular axes). However, it is interesting to observe from fig. 11 that as the simulation time increases instabilities clearly arises for $G = 0.8$. This means that

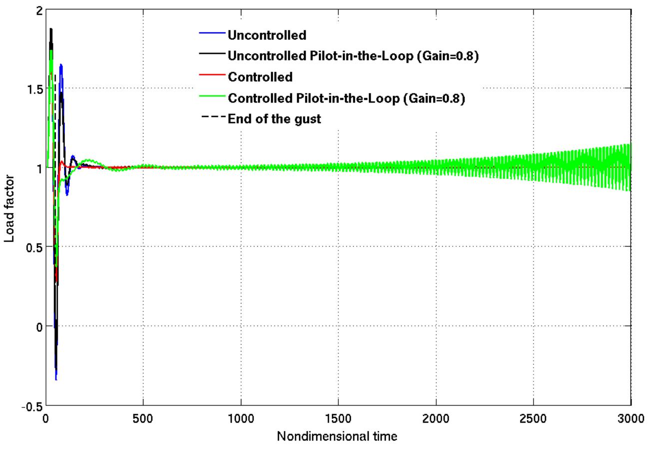

Fig. 11 Load factor due to $1-\cos$ gust, asymptotic behavior

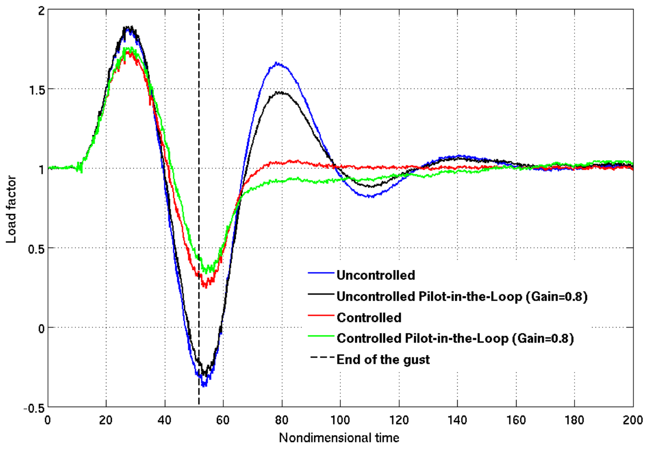

Fig. 13 Load factor due to stochastic gust, airplane mode

the controlled system becomes unstable when the pilot enters the loop. Therefore, it is demonstrated that a controller may couple adversely with pilot dynamics, thus yielding a divergent response. This result suggest the introduction of pilot in the loop in the simulation model used in the process of control law synthesis. In addition, fig. 12 shows the corresponding actuation of rotor controls: as expected in airplane mode, collective pitch is negligible without pilot in the loop, while it becomes significant when pilot effects are introduced. Finally, response to

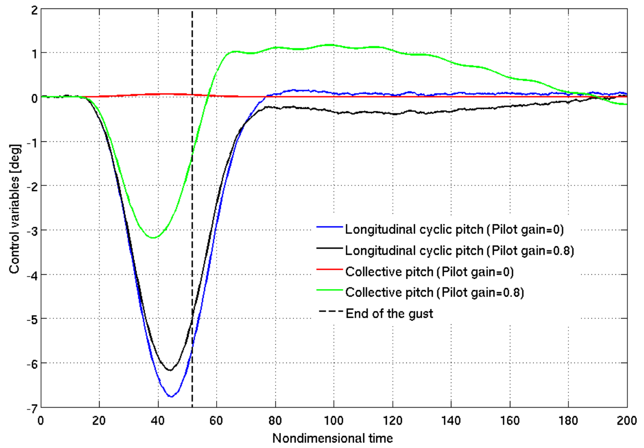

Fig. 12 Rotor controls history

stochastic gust and noise measurements is examined as for the helicopter-mode case. Figure 13 demonstrates that also in this case stochastic contributions do not particuarly affect control performance and tiltrotor-pilot coupling and Kalman filter is not affected negatively by the presence of the pilot.

6 Conclusions

In this work the influence of the inclusion of a pilot in a tiltorotor aeroelastic loop has been examined. In particular, the focus has been on the impact of his presence on a rotorcraft controlled through actuation laws synthetized without taking into account the pilot-in-the-loop effects. The test case has been a XV15-like tiltrotor with an optimal gust alleviation control coupled with a Kalman-Bucy filter. The pilot model applied has been the passive one developed by Mayo, suitable for mid frequency ($1-10$Hz) aeroelastic RPC analysis. Numerical results have shown two main interesting aspects in Automatic Flight Controls Systems-pilot coupling: first, pilot in the loop tends to reduce the amplitude of load factor peaks due to gust encounter, especially in helicopter mode flight; second, in some regions of the flight envelope (here in airplane mode), destabilizating interactions between AFCS and pilot may occur, hence suggesting the introduction of pilot modelling in the simulation tools that are used in the control design process.

7 Aknowledgments

This work has been supported by the Italian Ministry of University and Research (MIUR) under PRIN 2007-8TJFZE.

References

[1] Dieterich O, Goetz J, DangVu B, Haverdings H, Masarati P, Pavel M, Jump M, and Gennaretti M. Adverse rotorcraft-pilot coupling: Recent research activities in europe. *Proc of the 34th European Rotorcraft Forum (ERF)*, Liverpool, UK, 2008.

[2] Etkin B. *Dynamics of atmospheric flight*. Wiley, 1972.

[3] Fauchère P. Pio-pao, pilot induced-assisted oscillation. *Proc of the International Committee for Alpine Rescue congress (IKAR-CISA)*, Chamonix, France, 2008.

[4] Friedland B. *Control system design. An introduction to state-space methods*. McGraw-Hill, 1986.

[5] Gennaretti M and Bernardini G. Aeroelastic response of helicopter rotors using a 3-d unsteady aerodynamic solver. *The Aeronautical Journal*, Vol. 110, 2006.

[6] Gennaretti M, Molica Colella M, and Bernardini G. Analysis of tiltrotor airframe vibratory loads transmitted by the wing-proprotor system. *Proc of 9th Int'l Conference on Fluid-Induced Vibration (FIV)*, Prague, Czech Republic, 2008.

[7] Greenberg J. Airfoil in sinusoidal motion in a pulsating stream. Technical Report TN-1326, NACA, 1947.

[8] Hodges D and Dowell E. Nonlinear equation for the elastic bending and torsion of twisted nonuniform rotor blades. Technical Report TN D-7818, NASA, 1974.

[9] Johnson W. Analytical modeling requirements for tilting proprotor aircraft dynamics. Technical Report TN D-8013, NASA, 1975.

[10] Klyde D and Mitchell D. Investigating the role of rate limiting in pilot-induced oscillations. *Proc of the 47th AIAA Atmospheric Flight Mechanics Conference*, Austin, Texas, 2003.

[11] Masarati P, Quaranta G, Gennaretti M, and Serafini J. Aeroservoelastic analysis of rotorcraft-pilot coupling: a parametric study. *Proc of the 66th American Helicopter Society Annual Forum (AHS)*, Phoenix, Arizona, 2010.

[12] Masarati P, Quaranta G, Serafini J, and Gennaretti M. Numerical investigation of aeroservoelastic rotorcraft-pilot coupling. *Proc of the XIX AIDAA congress*, Forlí, Italy, 2007.

[13] Mayo J. The involuntary participation of a human pilot in a helicopter collective control loop. *Proc of the 15th European Rotorcraft Forum (ERF)*, Amsterdam, Netherlands, 1989.

[14] Muro D, Molica Colella M, and Gennaretti M. An optimal control approach for alleviation of tiltrotor gust response. *Proc of the XX AIDAA congress*, Milano, Italy, 2009.

[15] Parham Jr. T. V-22 pilot-in-the-loop aeroelastic stability analysis. *Proc of the 47th American Helicopter Society Annual Forum(AHS)*, Phoenix, Arizona, 1991.

[16] Serafini J, Gennaretti M, Masarati P, Quaranta G, and Dieterich O. Aeroelastic and biodynamic modeling for stability analysis of rotorcraft-pilot coupling phenomena. *Proc of the 34th European Rotorcraft Forum (ERF)*, Liverpool, UK, 2008.

[17] Serafini J, Greco L, and Gennaretti M. Reduced order aerodynamics modelling for rotorcraft-pilot coupling aeroelastic phenomena prediction. *Proc of the International Forum on Aeroelasticity and Structural Dynamics*, Seattle, Washington, 2009.

[18] Theodorsen T. General theory of aerodynamic instability and the mechanism of flutter. Technical Report Report 496, NACA, 1935.

8 Copyright Statement